Solar Energy xxx (xxxx) 112195

Contents lists available at ScienceDirect

Solar Energy

journal homepage: www.elsevier.com/locate/solener

Integration of a physics-based direct normal irradiance (DNI) model to enhance the National Solar Radiation Database (NSRDB)

Yu Xie [a], Manajit Sengupta [a], Jaemo Yang [a], Grant Buster [b], Brandon Benton [b], Aron Habte [a], Yangang Liu [c]

[a] Power Systems Engineering Center, National Renewable Energy Laboratory, Golden, CO 80401, United States
[b] Strategic Energy Analysis Center, National Renewable Energy Laboratory, Golden, CO 80401, United States
[c] Environmental and Climate Sciences Department, Brookhaven National Laboratory, Upton, NY 11973, United States

ARTICLE INFO

Keywords:
Solar radiation
DNI
NSRDB
Satellite data

ABSTRACT

The National Solar Radiation Database (NSRDB) is an extensively used dataset that furnishes satellite-retrieved solar resource data across the United States and an expanding list of other countries. Although the NSRDB uses a physical model to compute global horizontal irradiance (GHI), it currently employs an empirical approach based on surface observations to estimate cloudy-sky direct normal irradiance (DNI). Recently, a new physics-based approach, known as the Fast All-sky Radiation Model for Solar applications with DNI (FARMS-DNI), was developed to improve DNI forecasting. FARMS-DNI integrates direct and scattered solar radiances within the circumsolar region, resulting in improved day-ahead forecasting of DNI by incorporating it into the Weather Research and Forecasting model with Solar extensions (WRF-Solar). This study incorporates FARMS-DNI into the NSRDB algorithm to produce high-spatiotemporal-resolution DNI data from satellite data. The accuracy of the NSRDB based on FARMS-DNI is analyzed using surface observations from 19 sites situated within the National Oceanic and Atmospheric Administration (NOAA) Surface Radiation Budget (SURFRAD) and Solar Radiation (SOLRAD) networks, the University of Oregon (UO) network, the U.S. Department of Energy (DOE) Atmospheric Radiation Measurement (ARM) network, and at the National Renewable Energy Laboratory (NREL). The results demonstrate that FARMS-DNI reduces the significant overestimation of DNI in the conventional NSRDB at all surface sites, particularly in cloud overcast conditions classified using both satellite retrievals and surface observations. Consequently, this new model can effectively improve the overall accuracy of the NSRDB. The results also suggest that further improvement of DNI estimates at individual time steps, however, requires advanced satellite techniques and precise identification of clouds and retrieval of cloud properties.

1. Introduction

Global horizontal irradiance (GHI) and direct normal irradiance (DNI) are the most commonly used quantities for quantifying the magnitude of solar resource available at the earth's surface [9,15,21]. GHI represents the total amount of solar radiation in the downwelling direction from the atmosphere, whereas DNI represents the amount of solar radiation along the sun's direct path at a specific time [3,30]. Accurate modeling and forecasting of GHI and DNI are crucial for estimating the energy production of a solar power plant and integrating it into the electric grid. Compared to GHI, DNI is often more closely correlated with the production from a concentrating solar power (CSP) system or a photovoltaic (PV) tracking system. For example, the CSP models incorporated in the National Renewable Energy Laboratory's (NREL's) System Advisor Model (SAM) convert DNI and meteorological data into thermal energy, simulating the flow through system components while considering diverse losses, and subsequently transform the thermal energy into net electrical power [2].

The development of large-scale solar resource data depends on a combination of satellite observations and advanced modeling techniques to compute GHI and DNI. Empirical models develop regression functions that establish correlations between long-term satellite-based observations and surface-based measurements of solar radiation. The regression functions, in conjunction with satellite data, enable the estimation of GHI and DNI across various locations and time periods [4,6,14,20,28,29]. Physical models compute solar radiation by numerically solving the radiative transfer equation [5,18,24–26]. Satellite observations are used to retrieve meteorological properties such as cloud

Corresponding author.
E-mail address: yu.xie@nrel.gov (Y. Xie).

https://doi.org/10.1016/j.solener.2023.112195
Received 26 July 2023; Received in revised form 9 October 2023; Accepted 12 November 2023
0038-092/

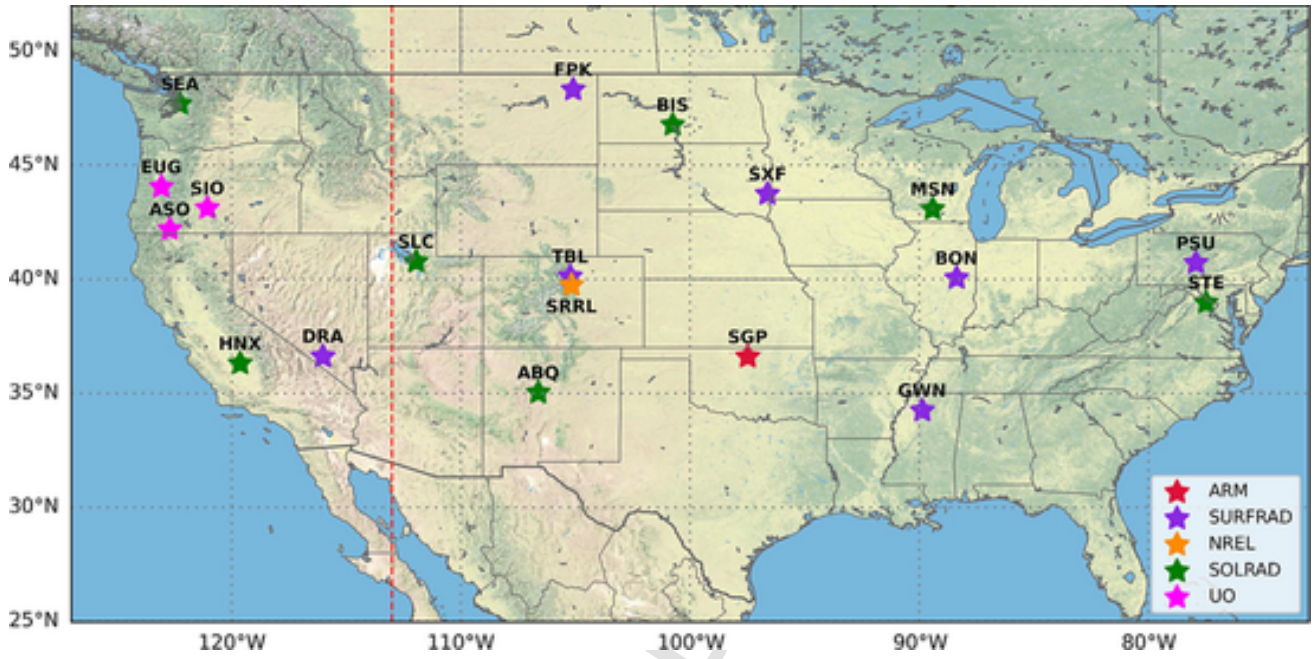

Fig. 1. The locations of the surface sites in the evaluation of DNI.

amount, cloud optical thickness, and cloud thermodynamic phase [11,12,16,27,38,39]. The satellite retrievals are combined with additional meteorological information from other sources to deduce the effects of absorption and scattering of solar radiation in the atmosphere [17,22].

Following the evaluation of satellite-based GHI and DNI data, it is commonly observed that DNI, derived through both empirical models and physical models, exhibits a larger bias than GHI [8,40,41]. This is mainly due to the fact that the light scattering in the forward direction is more sensitive to aerosol or cloud properties than in other directions [1,37]. As a result, minor uncertainties in the input data for a radiative transfer model can cause a significant bias in the computation of DNI while having only a limited impact on the GHI computation.

The current state-of-the-art parametric DNI models suffer from imperfections that can result in nonignorable bias in DNI computation. For instance, the Direct Insolation Simulation Code (DISC) [19] computes all-sky DNI using empirical relationships between surface observations of GHI and DNI. As a result, independent biases in the empirical relationships and GHI computation can compound and lead to a larger bias in DNI computation. Additionally, a specific GHI value can correspond to numerous combinations of the meteorological properties, each associated with a distinct DNI value. The consistent one-to-one match between GHI and DNI for a specific airmass can result in obvious errors in the DNI computation. The well-known Beer-Bouguer-Lambert law has been used by numerical weather prediction (NWP) models to compute direct solar radiation [18]. This algorithm ignores the scattered solar radiation within the circumsolar region and thus often leads to significant underestimation of DNI when used for solar forecasting [36]. The biases in the current DNI models were explicitly quantified through a comprehensive study utilizing 17 years of surface-based observations conducted at the Atmospheric Radiation Measurement (ARM) Southern Great Plain (SGP) site [34]. The findings revealed that DISC exhibited a significant overestimation of cloudy-sky DNI, with a bias of 153.85 %. The Beer-Bouguer-Lambert law underestimated the cloudy-sky DNI by 74.98 % and 78.85 for clouds composed of water droplets and ice crystals, respectively.

To address the limitations of the current DNI models, Xie et al. [34] developed a physics-based model, the Fast All-sky Radiation Model for Solar applications with DNI (FARMS-DNI), to efficiently infer all-sky solar radiation in the circumsolar region. This model has proved to be beneficial in reducing the bias in DNI forecasting when incorporated into the Weather Research and Forecasting model with Solar extensions (WRF-Solar) [13,36]. In this study, FARMS-DNI is integrated into the algorithm used to create the National Renewable Energy Laboratory's (NREL's) National Solar Radiation Database (NSRDB) [21]. The long-term DNI is calculated using FARMS-DNI and satellite data are validated using surface observations across the contiguous United States (CONUS).

2. A brief review of FARMS-DNI

FARMS is an efficient radiative transfer model computing broadband solar radiation on the earth's surface [33]. Under clear-sky conditions, it employs a clear-sky radiative transfer model, such as REST2 [7], to compute GHI and DNI. Under cloudy-sky conditions, the clear-sky radiative transfer model is used to compute the transmittance and reflectance of solar radiation in the cloud-free atmosphere. The computation is then combined with cloud transmittance and reflectance, parameterized based on a pre-computation for the possible cloud properties, to infer the cloudy-sky GHI. Note that the Beer-Bouguer-Lambert law significantly underestimates cloud transmittance for direct radiation because it does not account for the scattered radiation in the circumsolar region. To address this limitation, FARMS employs DISC to empirically compute cloudy-sky DNI from the GHI computation in the previous step. Because of the accurate and efficient computation of all-sky solar radiation, FARMS has been utilized to create long-term solar radiation data served by the NSRDB. It has also been integrated into WRF and WRF-Solar to provide high-resolution forecasts of solar radiation in the NWP systems.

FARMS has been updated with FARMS-DNI in the computation of cloudy-sky DNI [34]. The model can be expressed by the following equation:

$$DNI = F_0(T_{d0} + T_{d1} + T_{d2}) \quad (1)$$

where F_0 is the extraterrestrial solar irradiance, T_{d0} is the transmittance of the cloudy atmosphere in the infinite-narrow beam, T_{d1} is the transmittance related to the first-order scattered radiation in the circumsolar region, and T_{d2} is the transmittance related to the multiple reflection between cloud and land surface that falls into the circumsolar

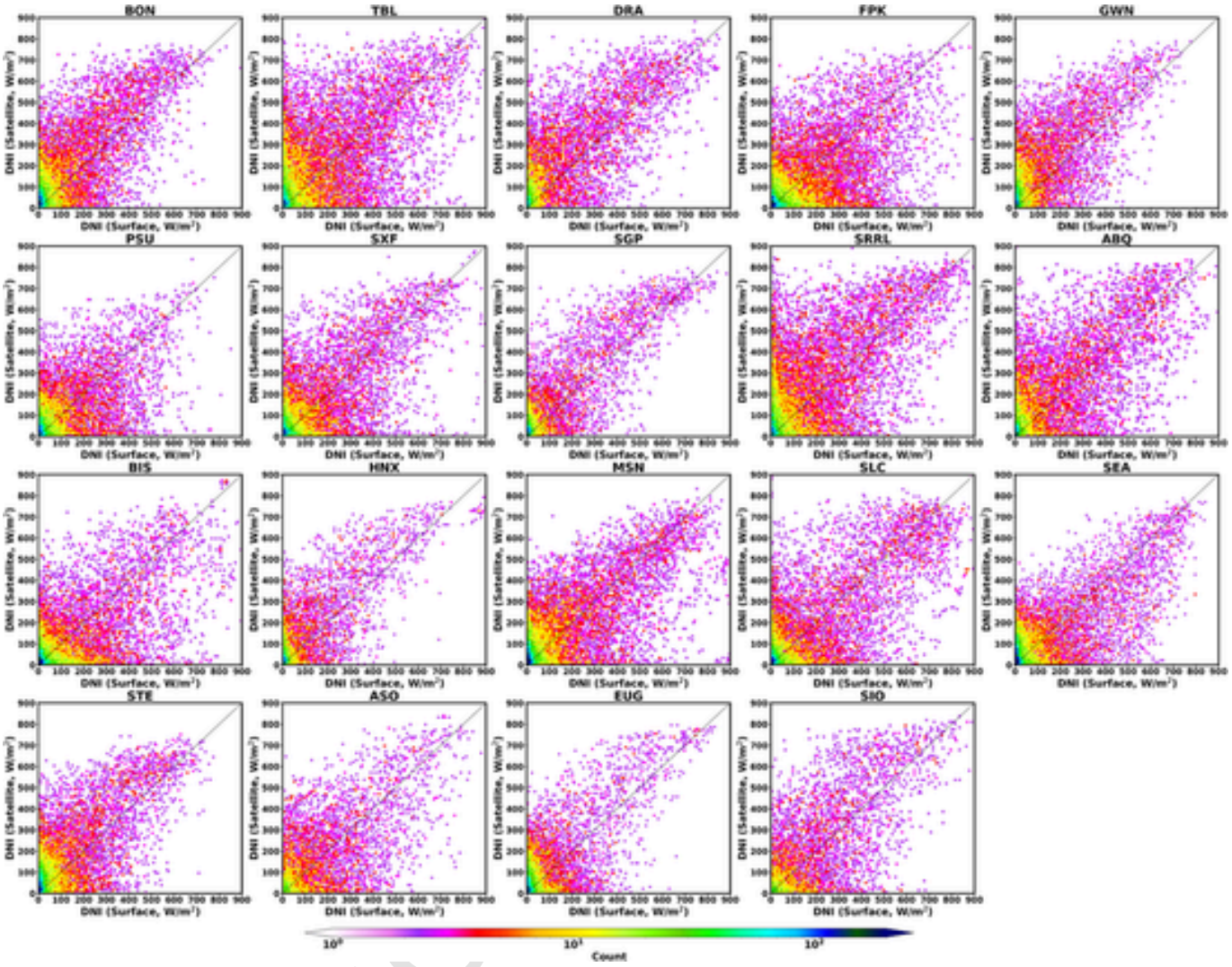

Fig. 2. Comparison of the cloudy-sky DNI between those computed by FARMS-DNI and surface observations.

region. The computation of T_{d0} is in accordance with the Beer-Bouguer-Lambert law using the clear-sky transmittance and the cloud optical thickness. T_{d1} can be derived through an integration of the solar radiances in the differential solid angles within the circumsolar region. T_{d2} is computed by the integration of the solar radiances reflected between the cloud and the land surface and then observed in the circumsolar region.

To express T_{d1} in Eq.(1), solar radiances in differential solid angles are inferred from a lookup table of cloud transmittances, calculated using the DIScrete Ordinates Radiative Transfer (DISORT) model [23] with various wavelengths, cloud properties and solar incident directions. For each solar zenith angle, solar radiances are computed in approximately 200 differential solid angles. These radiance values are integrated across the solar wavelengths and the circumsolar region to represent T_{d1}. This process is optimized through a parameterization of the cloud transmittances for the possible cloud properties and solar incident directions [42]. Yang et al. [42] discovered that the cloud transmittance can be accurately represented using the parameterization with a hyperbolic tangent function and determined coefficients. The DNI computed using FARMS-DNI with the parameterization closely matches the DNI computed using the precomputed cloud transmittances, while requiring significantly less computing time and memory usage. More details of FARMS-DNI are not reinstated in this context as they can be readily referenced in earlier literatures [34,42].

Note that FARMS-DNI is a physics-based model for computing cloudy-sky DNI, independent of regression or calibration based on surface observation of DNI, though a few approximations are made during the parameterization process. In contrast to DISC, which relies on a regression function derived from surface observation, FARMS-DNI exclusively utilizes physical properties of the atmosphere and land surface as its input. Consequently, this model is not limited by local climate conditions. When compared to the Beer-Bouguer-Lambert law, FARMS-DNI closely aligns with pyrheliometer observations because it includes scattered radiation within the circumsolar region.

FARMS-DNI coupled with the parameterization of cloud transmittance has been successfully integrated into WRF-Solar [36]. Compared to the Beer-Bouguer-Lambert law adopted by the conventional WRF-Solar, the forecasting of day-ahead DNI over 9-km grid boxes is significantly improved by FARMS-DNI, as validated using 1-year surface-based observations and satellite data. More specifically, the use of FARMS-DNI reduces the percentage error (PE) of the DNI forecasting over Table Mountain, Colorado from −28.62 % to –0.59 %. For CONUS, the average PE over satellite pixels is reduced from −54.39 % to −14.08 %. Given these results, it would be interesting to investigate whether integrating FARMS-DNI into the NSRDB algorithm could provide benefits for the satellite-based resource assessment of DNI.

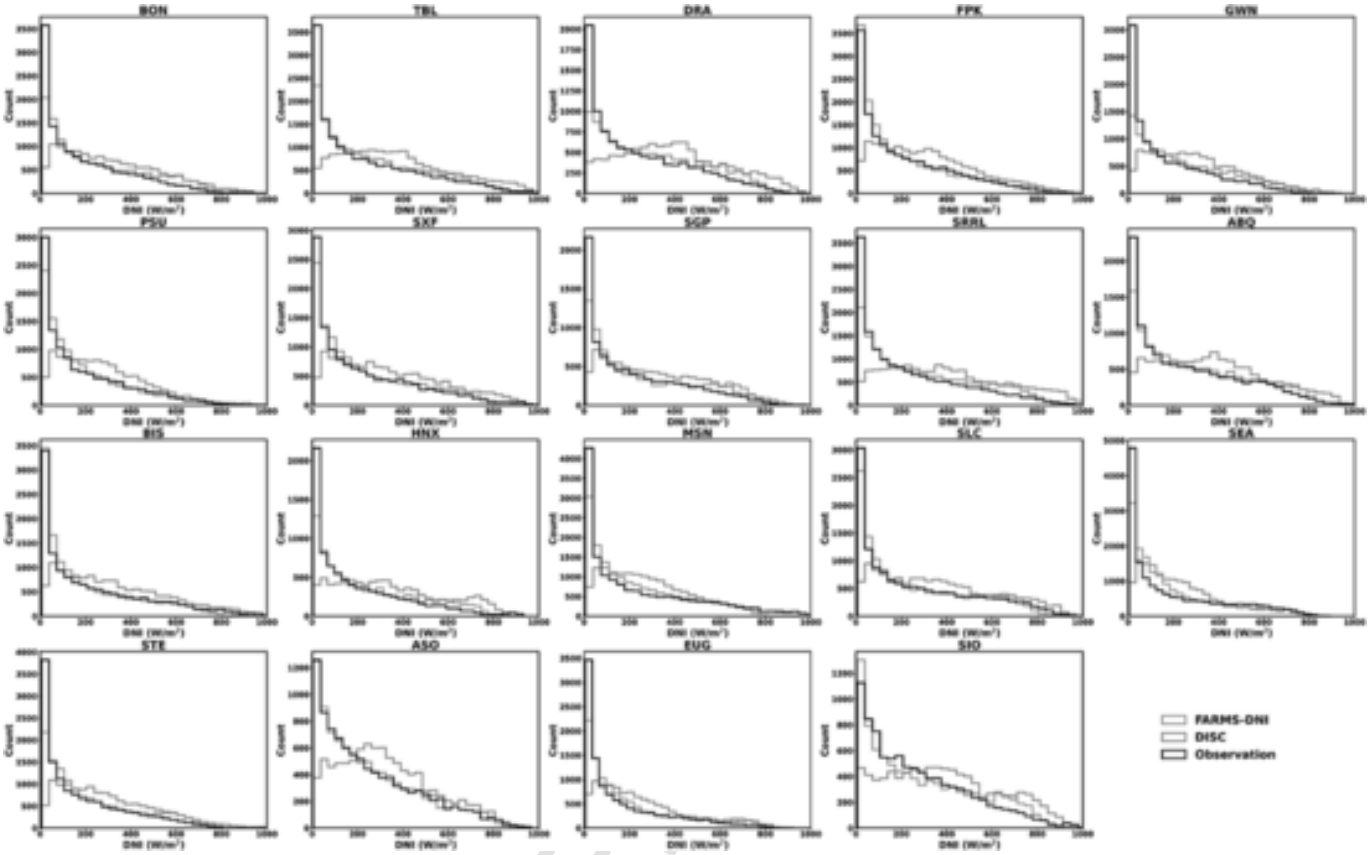

Fig. 3. The distribution of the cloudy-sky DNI observed at the land surface and those computed using FARMS-DNI and DISC.

3. Integration of FARMS-DNI into the NSRDB

The NSRDB is one of the most often used solar resource data sets for solar energy applications and other purposes [21]. With the users' selection of spatial and temporal coverages, solar radiation and with other meteorological products—such as surface temperature and wind speed—can be downloaded through NREL's server, an application programming interface (API) service, or the Amazon Web Services (AWS) cloud services. In addition to GHI, DNI, and diffuse horizontal irradiance (DHI), users can also access hyperspectral solar data for specific photovoltaic (PV) surfaces with various orientations [31,32,35]. For CONUS, the NSRDB employs data from the Geostationary Operational Environmental Satellite (GOES), the Modern-Era Retrospective analysis for Research and Applications, Version 2 (MERRA-2), and other ancillary data to assess solar radiation at each 30-minute interval from 1998 to 2018, with a spatial resolution of 4 km. Since 2019, the NSRDB data have been available at a higher temporal resolution of 5 min and an improved spatial resolution of 2 km.

In this study, the NSRDB algorithm is enhanced with the integration of FARMS-DNI, coupled with the new parameterization of cloud transmittance. The clear-sky DNI is consistent with the conventional NSRDB, where REST2 is used to compute both clear-sky GHI and DNI. For cloudy-sky conditions, a sequential computation by FARMS and DISC is substituted by a concurrent procedure that utilizes satellite cloud products to infer cloud transmittance and reflectance for both direct and total downwelling solar radiation. The cloud transmittance and reflectance are then incorporated with FARMS, FARMS-DNI and the clear-sky computation to resolve the cloudy-sky GHI and DNI.

Following the algorithm, all-sky DNIs near 19 surface sites in the networks of the Surface Radiation Budget (SURFRAD), Solar Radiation (SOLRAD), the University of Oregon (UO), the U.S. Department of Energy ARM, and NREL are computed using the NSRDB input data for each 5-minute interval during 2019–2020. Fig. 1 displays the locations of the surface sites considered in the study. The SURFRAD network consists of 7 sites at Bondville, Illinois (BON); Desert Rock, Nevada (DRA); Goodwin Creek, Mississippi (GWN); Fort Peck, Montana (FPK); the Pennsylvania State University (PSU); Sioux Falls, South Dakota (SXF); and Table Mountain, Colorado (TBL). The SOLRAD network includes sites in Albuquerque, New Mexico (ABQ); Bismarck, North Dakota (BIS); Hanford, California (HNX); Madison, Wisconsin (MSN); Salt Lake City, Utah (SLC); Seattle, Washington (SEA); and Sterling, Virginia (STE). The UO network includes 3 sites: Ashland, Oregon (ASO); Eugene, Oregon (EUG); and Silver Lake, Oregon (SIO). The ARM and NREL sites are located at the SGP and Solar Radiation Research Laboratory (SRRL), respectively. Following the NSRDB algorithm, the DNI in the west and east of the red line (-113° longitude) in Fig. 1 is computed using GOES-17 and GOES-16 data, respectively. For comparison with FARMS-DNI, DNI is also computed using the conventional NSRDB algorithm, where DISC is used to compute DNI from the GHI simulated by FARMS.

4. Validation

To assess the accuracy of FARMS-DNI in the NSRDB processing, the computed DNI based on the satellite data are validated using surface observations. To align with the time steps of the NSRDB, the 1-minute resolution surface observations are first averaged over each 5-minute interval around the corresponding NSRDB timestamp. Building on prior research efforts [10,40,41], data quality control is performed to eliminate extreme conditions. Additionally, we incorporated certain variations in the criteria for DNI that are associated with limited solar energy but present substantial uncertainties in percentage. The data quality control involves excluding data when (1) the solar zenith angle is larger than 80°; (2) the surface observed GHI is smaller than 50 W/m^2; (3) the

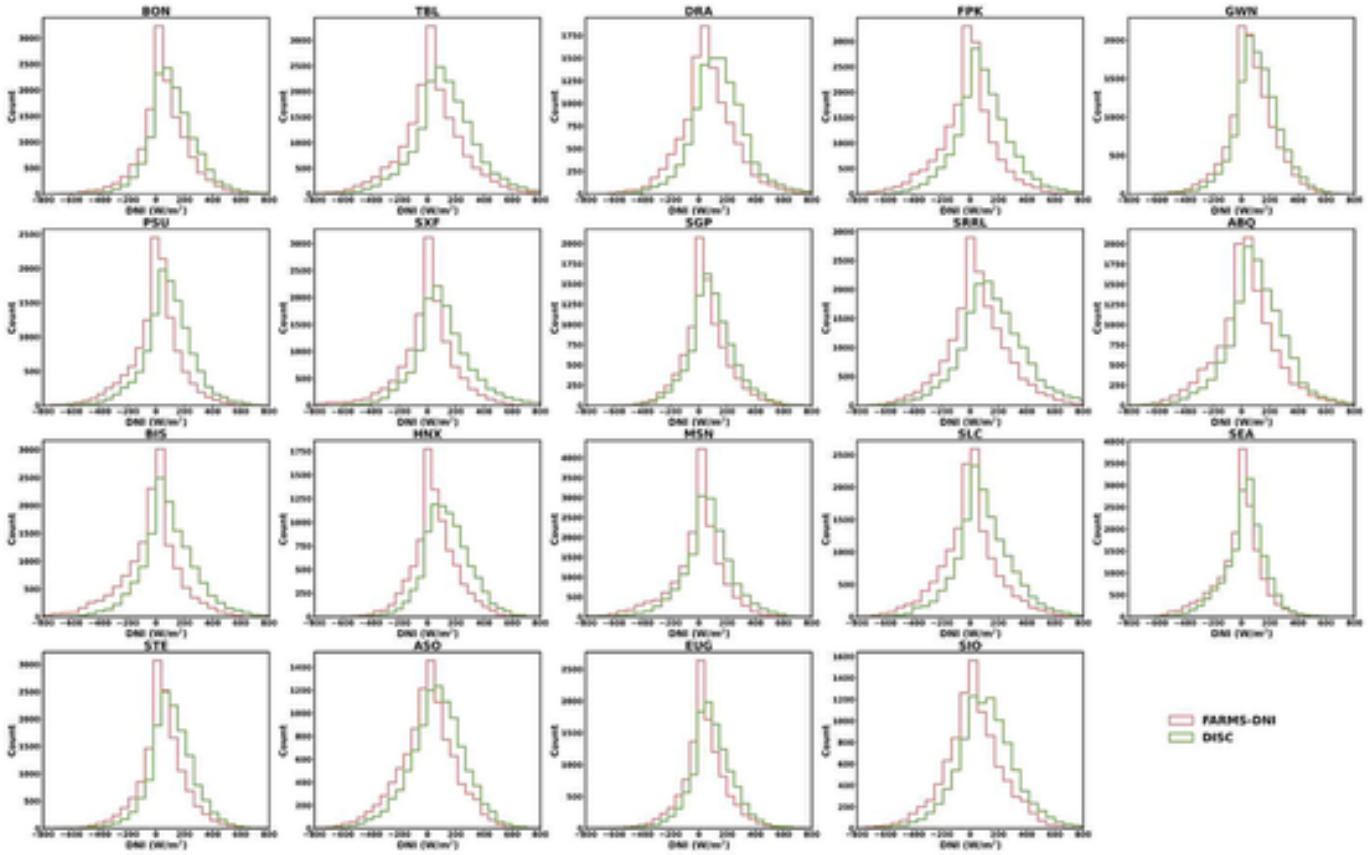

Fig. 4. The bias of the cloudy-sky DNI computed by FARMS-DNI and DISC.

surface observed DNI is smaller than 5 W/m²; or (4) the computed DNI is smaller than 5 W/m². Cloudy-sky scenes are identified based on the following criteria: (1) they are classified as cloudy-sky conditions by the GOES cloud product; (2) the surface observed GHI is smaller than the clear-sky GHI computed using REST2; and (3) the surface observed DNI is smaller than the clear-sky DNI computed using REST2. The criteria above ensure inclusion of cloudy-sky scenes by using a combination of satellite data and surface observations. It is important to acknowledge the potential for bias arising from the application of REST2 and the related input data [40]. For example, scenes containing extremely thin cirrus clouds can be inadvertently excluded when REST2 underestimates the clear-sky GHI and DNI. This can lead to a reduction of the sample size for cloudy-sky conditions. However, criteria (2) and (3) significantly reduce the bias in the cloud identification by the satellites and thus are implemented in this study.

Fig. 2 illustrates the cloudy-sky DNI computed using FARMS-DNI for the period from 2019 to 2020 compared to the surface observations from the 19 surface sites in the previously mentioned networks. The distribution of cloudy-sky DNI is skewed towards the lower-intensity region due to the light scattering and absorption by clouds. The cloudy-sky DNI greater than 400 W/m² are usually associated with thin clouds where the light scattering around the forward direction is more significant than the other directions. The distribution of cloudy-sky DNIs is mostly centered around the 1:1 line, indicating good overall agreement between the computation by FARMS-DNI and the surface observations. However, bias is noticeable in the individual computations. According to the Beer-Bouguer-Lambert law, direct radiation in an infinite-narrow beam is an exponential function of cloud optical thickness, suggesting that the bias in satellite-based cloud products is usually significantly amplified when they are used to compute DNI. Therefore, an accurate cloud retrieval technique is as important as the radiative transfer model in the DNI computation.

Fig. 3 shows the distribution of the cloudy-sky DNI observed at the land surface, and as computed using FARMS-DNI and DISC. Notably, DISC substantially underestimates the concentration of DNI in the lower-intensity region while overestimating it in the higher-intensity region. The observation suggests that DISC tends to overestimate most cloudy-sky DNI. This aligns with the findings of a prior study by Xie et al. [34], where cloudy scenes were identified using surface-based total sky imaging data at ARM SGP and NREL SRRL. The overestimation by DISC is probably caused by the regression functions that are determined for all-sky conditions. When this method is applied to GHI in cloud overcast conditions, it tends to assume a compounding of clear-sky and cloudy-sky conditions and thus overestimates the cloudy-sky DNI. Compared to DISC, FARMS-DNI has a better agreement with the surface observation of the cloudy-sky DNI. This is also shown in Fig. 4, which displays the bias of the cloudy-sky DNI computed by FARMS-DNI and DISC. A more comprehensive diagnose of bias by DISC and FARMS-DNI requires a meticulous analysis that takes into account specific cloud conditions. For example, FARMS-DNI is specifically designed for cloud overcast conditions, which means it may exhibit more significant bias when faced with limited cloud cover. Conversely, DISC might present larger bias in cloudy-sky conditions because the regression function was determined in all-sky conditions. To further pinpoint the underlying reasons for bias, it is imperative to rely on accurate cloud property data, encompassing parameters such as cloud optical thickness, cloud particle size, cloud thermodynamic phase, and cloud fraction. Ongoing research efforts are dedicated to advancing our understanding in this domain.

To quantitively assess the bias of FARMS-DNI and DISC, we consider 4 metrics: mean bias error (MBE), mean absolute error (MAE), percentage error (PE), and absolute percentage error (APE)— which are defined as follows:

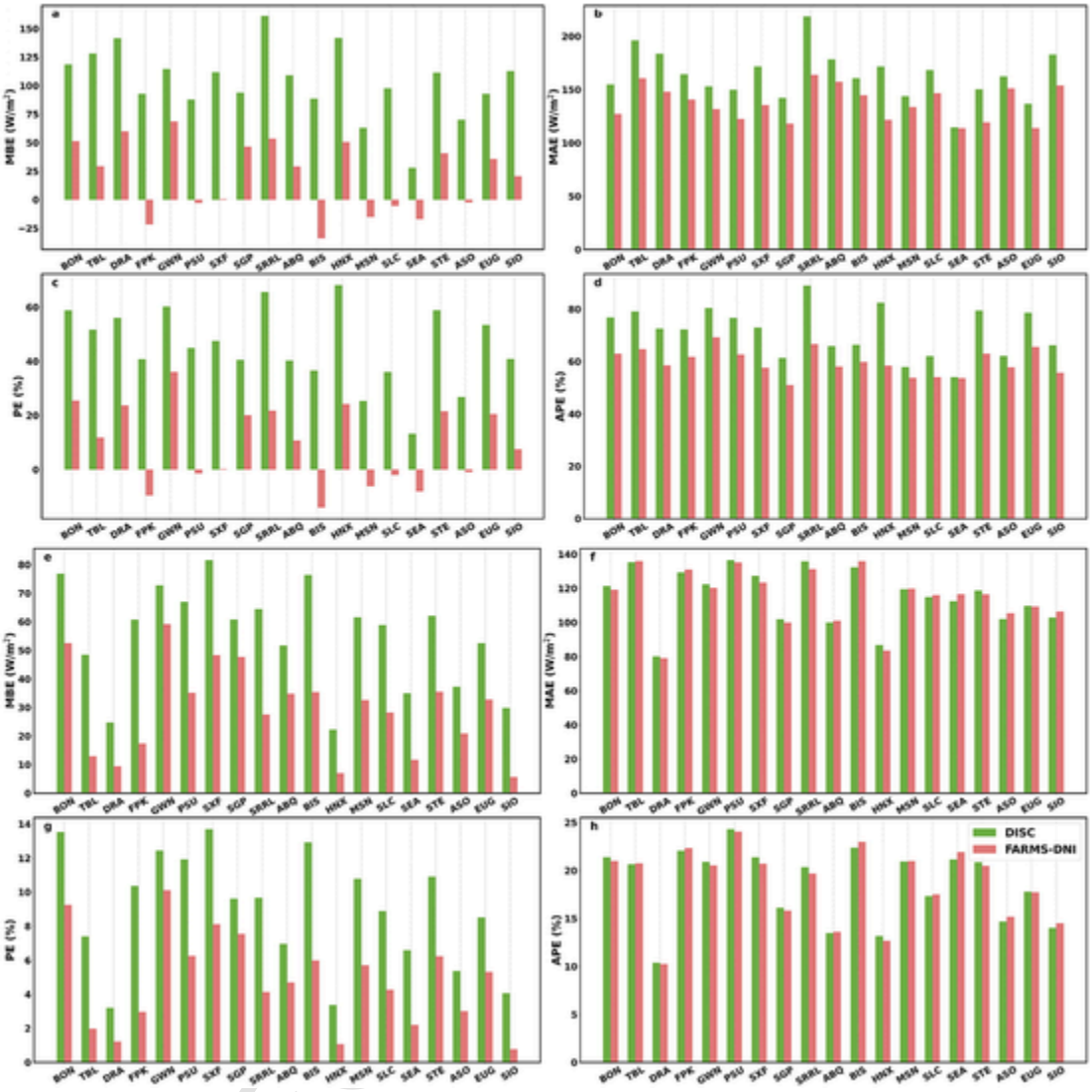

Fig. 5. (a-d) The error metrics of the cloudy-sky DNI and (e-h) those of the all-sky DNI computed by DISC and FARMS-DNI.

$$\mathrm{MBE} = \frac{1}{n}\sum_{i=1}^{n}(DNI_M - DNI_O) \tag{2a}$$

$$\mathrm{MAE} = \frac{1}{n}\sum_{i=1}^{n}\left|DNI_M - DNI_O\right| \tag{2b}$$

$$\mathrm{PE} = \frac{\sum_{i=1}^{n}(DNI_M - DNI_O)}{\sum_{i=1}^{n} DNI_O} \times 100\% \tag{2c}$$

$$\mathrm{APE} = \frac{\sum_{i=1}^{n}\left|DNI_M - DNI_O\right|}{\sum_{i=1}^{n} DNI_O} \times 100\% \tag{2d}$$

where n is the number of the cloudy-sky scenarios, and the subscripts "M" and "O" denote the model simulation and surface-based observation, respectively. Fig. 5a-5d shows the metrics of the cloudy-sky DNI computed by DISC and FARMS-DNI. The MBE and PE indicate that DISC overestimates cloudy-sky DNI at all the sites, which is attributed to both the DISC model and the computation of cloudy-sky GHI. However, using FARMS-DNI can moderate this bias, particularly for sites with high occurrences of snow and bright surfaces such as TBL, SRRL, DRA, and HNX. The overestimation of DNI is converted to a slight underestimation in a few sites, leading to an even lower bias in the average over all 19 sites. In addition, the use of FARMS-DNI reduces the MAE and APE of the cloudy-sky DNI, as shown in Fig. 5b and 5d. Fig. 5e-5 h presents the error metrics of the all-sky DNI, including clear-sky and near-clear-sky conditions, which were excluded using the previously mentioned criteria. The cloudy-sky computation is performed by DISC and FARMS-DNI, whereas the clear-sky DNI is given by REST2. The results show that FARMS-DNI outperforms DISC in terms of MBE and PE for the all-sky DNI. Moreover, the MAE and APE of DISC and FARMS-DNI are comparable over the 19 surface sites. Based on the improved accuracy in both the cloudy-sky and all-sky conditions, as demonstrated in Fig. 5, integrating FARMS-DNI into the NSRDB algorithm is expected to enhance the DNI data.

5. Conclusions

This study aims to improve satellite-based DNI data by integrating a physical model, FARMS-DNI, into the NSRDB developing algorithm. The FARMS-DNI model numerically computes cloudy-sky DNI by integrating the infinite-narrow beam associated with the Beer-Bouguer-Lambert law, the first-order scattered radiation in the circumsolar region, and the multiple scattering between cloud and land surface that falls into the circumsolar region. A parameterization of the cloud transmittance for direct solar radiation is utilized to improve the computational efficiency of FARMS-DNI, based on our previous studies.

To evaluate the accuracy of the new model, cloudy-sky DNI was computed using FARMS-DNI, along with a combination of GOES satellite data, MERRA-2, and other ancillary data. The evaluation is conducted using 2-year surface-based observations over 19 sites across CONUS. The results show that DISC used in the conventional NSRDB severely overestimated DNI at all sites when the atmosphere is confidently cloudy. This bias is significantly reduced by FARMS-DNI, which is specifically designed for cloud overcast scenarios. FARMS-DNI also evidently improve the all-sky DNI from the conventional NSRDB. Therefore, integrating FARMS-DNI into the NSRDB algorithm is expected to enhance the accuracy of the DNI data.

Note that FARMS-DNI still shows substantial bias in the individual cloudy-sky scenarios even though it reduces the overall uncertainty in the long-term averaged data. This comes likely from a joint effect of the model bias and the bias in the satellite-based cloud retrievals. Because DNI is particularly sensitive to cloud optical thickness, it is crucial to further improve cloud retrieval techniques and utilize them in future DNI computations. Additionally, the performance of DISC and FARMS-DNI in partially cloudy conditions requires further investigation, even though FARMS-DNI shows better performance in all-sky and confidently cloudy conditions. Accurate cloud coverage data play an important role in computing cloudy-sky DNI because FARMS-DNI is designed for cloud overcast conditions. The use of precise cloud coverage data from advanced satellite technique, such as the improved spatial resolution provided by GOES-16 and GOES-17, should aid in further improving DNI assessment.

Declaration of Competing Interest

The authors declare that they have no known competing financial interests or personal relationships that could have appeared to influence the work reported in this paper.

Acknowledgments

This work was authored in part by the National Renewable Energy Laboratory, operated by Alliance for Sustainable Energy, LLC, for the U.S. Department of Energy (DOE) under Contract No. DE-AC36-08GO28308. Funding provided by the U.S. Department of Energy Office of Energy Efficiency and Renewable Energy Solar Energy Technologies Office and the Office of Science Atmospheric System Research program. The Brookhaven National Laboratory is operated by the Brookhaven Science Associates, LLC (BSA), for the U.S. Department of Energy under Contract No. DE-SC0012704.

The views expressed in the article do not necessarily represent the views of the Department of Energy or the U.S. Government. The U.S. Government retains and the publisher, by accepting the article for publication, acknowledges that the U.S. Government retains a nonexclusive, paid-up, irrevocable, worldwide license to publish or reproduce the published form of this work, or allow others to do so, for U.S. Government purposes.

This research was performed using computational resources sponsored by the Department of Energy's Office of Energy Efficiency and Renewable Energy and located at the National Renewable Energy Laboratory.

References

Baum, B.A., Yang, P., Heymsfield, A.J., Schmitt, C.G., Xie, Y., Bansemer, A., Hu, Y.X., Zhang, Z.B., 2011. Improvements in shortwave bulk scattering and absorption models for the remote sensing of ice clouds. J. Appl. Meteorol. Clim. 50, 1037–1056.

Blair, N., Dobos, A., Freeman, J., Neises, T., Wagner, M., Ferguson, T., Gilman, P., Janzou, S., 2014. System Advisor Model, SAM 2014.1. 14: General description. National Renewable Energy Laboratory, Golden, CO.

Blanc, P., Espinar, B., Geuder, N., Gueymard, C., Meyer, R., Pitz-Paal, R., Reinhardt, B., Renne, D., Sengupta, M., Wald, L., Wilbert, S., 2014. Direct normal irradiance related definitions and applications: The circumsolar issue. Sol. Energy 110, 561–577.

Cano, D., Monget, J., Albuisson, M., Guillard, H., Regas, N., Wald, L., 1986. A method for the determination of the global solar radiation from meteorological satellite data. Sol. Energy 37, 31–39.

Chandrasekhar, S., 1950. Radiative transfer. Oxford Univ. Press, Oxford.

Feng, L., Lin, A., Wang, L., Qin, W., Gong, W., 2018. Evaluation of sunshine-based models for predicting diffuse solar radiation in China. Renew. Sustain. Energy Rev. 94, 168–182.

Gueymard, C., 2008. REST2: High-performance solar radiation model for cloudless-sky irradiance, illuminance, and photosynthetically active radiation - Validation with a benchmark dataset. Sol. Energy 82 (3), 272–285.

Gueymard, C., Ruiz-Arias, J., 2016. Extensive worldwide validation and climate sensitivity analysis of direct irradiance predictions from 1-min global irradiance. Sol. Energy 128, 1–30.

Gurtuna, O., Prevot, A., 2011. An overview of solar resource assessment using meteorological satellite data. Recent Advances in Space Technologies (RAST), 2011 5th International Conference on 10.1109/RAST.2011.5966825, 209 - 212.

Habte, A., Sengupta, M., Lopez, A., 2017. Evaluation of the National Solar Radiation Database (NSRDB): 1998–2015 National Renewable Energy Laboratory, Golden, CO.

Huang, G., Li, Z., Li, X., Liang, S., Yang, K., Wang, D., Zhang, Y., 2019. Estimating surface solar irradiance from satellites: Past, present, and future perspectives. Remote Sens. Environ. 233, 111371.

Husi, L., Nagao, T., Nakajima, T., Riedi, J., Ishimoto, H., Baran, A., Shang, H., Sekiguchi, M., Kikuchi, M., 2018. Ice cloud properties from Himawari-8/AHI next-generation geostationary satellite: Capability of the AHI to monitor the DC cloud generation process. IEEE Trans. Geosci. Remote Sens. 1–11.

Jimenez, P., Hacker, P., Dudhia, J., Haupt, S., Ruiz-Arias, J., Gueymard, C., Thompson, G., Eidhammer, T., Deng, A., 2016. WRF-Solar: Description and clear-sky assessment of an augmented NWP model for solar power prediction. Bull. Amer. Meteor. Soc. 97, 1249–1264.

Justus, C., Paris, M., Tarpley, J., 1986. Satellite-measured insolation in the United States, Mexico, and South America. Remote Sens. Environ. 20 (1), 57–83.

Kleissl, J., 2013. Solar energy forecasting and resource assessment. Academic Press.

Letu, H., Nakajima, T., Wang, T., Shang, H., Ma, R., Yang, K., Baran, A., Riedi, J., Ishimoto, H., Yoshida, M., Shi, C., Khatri, P., Du, Y., Chen, L., Shi, J., 2022. A new benchmark for surface radiation products over the East Asia-Pacific region retrieved from the Himawari-8/AHI next-generation geostationary satellite. Bull. Amer. Meteor. Soc. 103, 873–888.

Li, J., Tang, W., Yang, K., Xie, Y., Gueymard, C., Qin, J., Sengupta, M., 2021. An improved algorithm for estimating surface shortwave radiation: Preliminary evaluation with MODIS products. IEEE Trans. Geosci. Remote Sens. https://doi.org/10.1109/TGRS.2021.3098742.

Liou, K.N., 2002. An introduction to atmospheric radiation, 2nd ed. Academic Press, Amsterdam, Boston.

Maxwell, E., 1987. A quasi-physical model for converting hourly global horizontal to direct normal insolation. Solar Energy Research Inst, Golden CO.

Perez, R., Ineichen, P., Moore, K., Kmiecik, M., Chain, C., George, R., Vignola, F., 2002. A new operational model for satellite-derived irradiances: Description and validation. Sol. Energy 73 (5), 307–317.

Sengupta, M., Xie, Y., Lopez, A., Habte, A., Maclaurin, G., Shelby, J., 2018. The National Solar Radiation Data Base (NSRDB). Renew. Sustain. Energy Rev. 89, 51–60.

Shi, H., Li, W., Fan, X., Zhang, J., Hu, B., Husi, L., Shang, H., Han, X., Song, Z., Zhang, Y., Wang, S., Chen, H., Xia, X., 2018. First assessment of surface solar irradiance derived from Himawari-8 across China. Sol. Energy 174, 164–170.

Stamnes, K., Tsay, S.C., Wiscombe, W., Jayaweera, K., 1988. Numerically stable algorithm for discrete-ordinate-method radiative transfer in multiple scattering and emitting layered media. Appl. Opt. 27 (12), 2502–2509.

Sun, Z., Li, J., He, Y., Li, J., Liu, A., Zhang, F., 2016. Determination of direct normal irradiance including circumsolar radiation in climate/NWPmodels. Q. J. R. Meteorol. Soc. 142, 2591–2598.

Sun, Z., Li, J., Shi, G., Manners, J., Li, J., 2020. Fast scheme for determination of direct normal irradiance. Part II: Parameterization of circumsolar radiation. Sol. Energy 199, 256–267.

Sun, Z., Liu, A., 2013. Fast scheme for estimation of instantaneous direct solar irradiance at the Earth's surface. Sol. Energy 98, 125–137.

Tana, G., Ri, X., Shi, C., Ma, R., Letu, H., Xu, J., Shi, J., 2023. Retrieval of cloud microphysical properties from Himawari-8/AHI infrared channels and its application in surface shortwave downward radiation estimation in the sun glint region. Remote Sens. Environ. 290, 113548.

Wang, L., Kisi, O., Zounemat-Kermani, M., Salazar, G., Zhu, Z., Gong, W., 2016. Solar radiation prediction using different techniques: modle evaluation and comparison. Renew. Sustain. Energy Rev. 61, 384–397.

Wang, L., Lu, Y., Zou, L., Feng, L., Wei, J., Qin, W., Niu, Z., 2019. Prediction of diffuse solar radiation based on multiple variables in China. Renew. Sustain. Energy Rev. 103, 151–216.

WMO, 2010. CIMO guide to meteorological instruments and methods of observation, Measurement of radiation. World Meteorological Organization, Geneva, Switzerland.

Xie, Y., Sengupta, M., 2018. A Fast All-sky Radiation Model for Solar applications with Narrowband Irradiances on Tilted surfaces (FARMS-NIT): Part I. The clear-sky model. Sol. Energy 174, 691–702.

Xie, Y., Sengupta, M., Dooraghi, M., 2018. Assessment of uncertainty in the numerical simulation of solar irradiance over inclined PV panels: New algorithms using measurements and modeling tools. Sol. Energy 165, 55–64.

Xie, Y., Sengupta, M., Dudhia, J., 2016. A Fast All-sky Radiation Model for Solar applications (FARMS): Algorithm and performance evaluation. Sol. Energy 135, 435–445.

Xie, Y., Sengupta, M., Liu, Y., Long, H., Min, Q., Liu, W., Habte, A., 2020. A physics-based DNI model assessing all-sky circumsolar radiation. iScience 22, doi.org/10.1016/

j.isci.2020.100893.

Xie, Y., Sengupta, M., Wang, C., 2019. A Fast All-sky Radiation Model for Solar applications with Narrowband Irradiances on Tilted surfaces (FARMS-NIT): Part II. The cloudy-sky model. Sol. Energy 188, 799–812.

Xie, Y., Yang, J., Sengupta, M., Liu, Y., Zhou, X., 2022. Improving the prediction of DNI with physics-based representation of all-sky circumsolar radiation. Sol. Energy 231, 758–766.

Xie, Y., Yang, P., Kattawar, G.W., Baum, B., Hu, Y.X., 2011. Simulation of the optical properties of ice particle aggregates for application to remote sensing of cirrus clouds. Appl. Opt. 50, 1065–1081.

Xie, Y., Yang, P., Kattawar, G.W., Minnis, P., Hu, Y.X., 2009. Effect of the inhomogeneity of ice crystals on retrieving ice cloud optical thickness and effective particle size. J. Geophys. Res. 114, D11203, doi:11210.11029/12008JD011216.

Xie, Y., Yang, P., Kattawar, G.W., Minnis, P., Hu, Y.X., Wu, D., 2012. Determination of ice cloud models using MODIS and MISR data. Int. Remote Sens. 33, 4219–4253.

Yang, D., 2021. Validation of the 5-min irradiance from the National Solar Radiation Database (NSRDB). J. Renew. Sustain. Energy 13. https://doi.org/10.1063/1065.0011635.

Yang, D., Bright, J., 2020. Worldwide validation of 8 satellite-derived and reanalysis solar radiation products: A preliminary evaluation and overall metrics for hourly data over 27 years. Sol. Energy 3–19.

Yang, J., Xie, Y., Sengupta, M., Liu, Y., Long, H., 2022. Parameterization of cloud transmittance for expeditious assessment and forecasting of all-sky DNI. J. Renew. Sustain. Energy 14, 063703.